JOURNAL OF MATERIALS SCIENCE 16 (1981) 649–659

# On fibre debonding effects and the mechanism of transverse-ply failure in cross-ply laminates of glass fibre/thermoset composites

J. E. BAILEY, A. PARVIZI
*Department of Metallurgy and Materials Technology, University of Surrey, Guildford, England*

The mechanism of transverse-ply failure in cross-ply laminates of glass fibre thermoset composites has been investigated. It is shown that fibre debonding initiates failure, the debonds subsequently joining up to form a transverse crack nucleus. In the epoxy system investigated fibre debonding causes an observable whitening effect and small modulus change; this effect is reversible in that rebonding can be brought about by further heat treatment. It is shown that in the case of the polyester system the larger thermal strains introduced during the curing cycle cause debonding of the composite and therefore the whitening effects are not observed on application of load. Simple models for the prediction of the observed effect of glass fibre volume fraction on transverse failure strain are proposed.

## 1. Introduction

In a recent paper [1] describing the behaviour of $0°/90°/0°$ glass fibre epoxy cross-ply laminates a small modulus change was reported at a strain lower than that at which transverse cracking initiated; associated with this phenomenon was a visual, under some circumstances, reversible, whitening effect.

This paper describes further investigations of the whitening effect and describes experiments demonstrating further the reversible nature of the effect. The studies are extended to include glass fibre polyester material, and the effect of fibre volume fraction on the transverse tensile strength of single-ply laminates is investigated.

## 2. Experimental procedure

$90°$ unidirectional and $0°/90°/0°$ cross-ply laminates were subjected to conventional tensile tests and to structural studies by scanning electron microscopy while the specimen was under load. For the latter part of the work, a strain stage was especially designed and built to fit a "TV" mini scanning electron microscope [2]. Both monotonic and cyclic loading tests accompanied by annealing of the specimen in between some of the cycles, were carried out on the specimens.

The main part of this work was performed on laminates, see Fig. 1a, made of "E" glass fibre roving (Silenka 1200 TEX silane heated) reinforcing an epoxy resin (Shell Epikot 828 cured with 80 parts per hundred of resin (pph) of Epikure NMA and 0.5 pph accelerator BDMA). However, some laminates were also made of glass fibre in a polyester resin (Scott Bader Crystic 390 mixed with 2 pph of catalyst MEKP and 0.2 pph cobalt napthate accelerator). The curing schedule for the epoxy laminates was 3 h at $100°$ C followed by 4 h of post-cure at $150°$ C. For polyester laminates the cure procedure was 24 h at room temperature followed by 3 h at $80°$ C. These laminates were built up using open metallic frames as described elsewhere [3].

The unidirectional composites had a varying fibre volume fraction, $V_f$. In order to investigate the effect of fibre packing on the ply's transverse

0022–2461/81/030649–11$03.10/0  

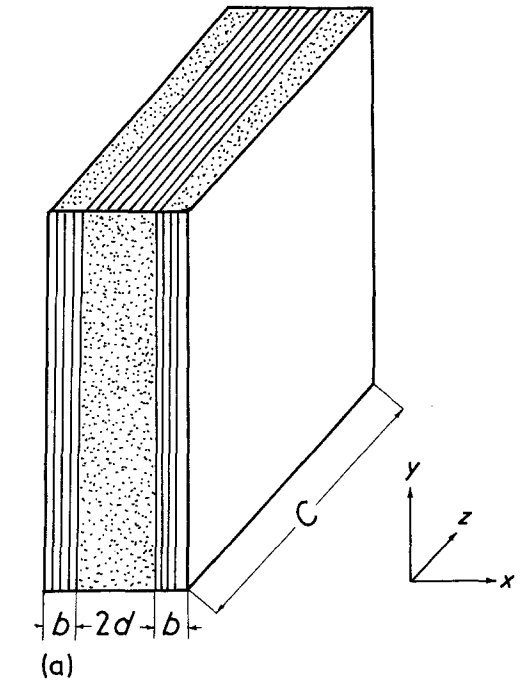


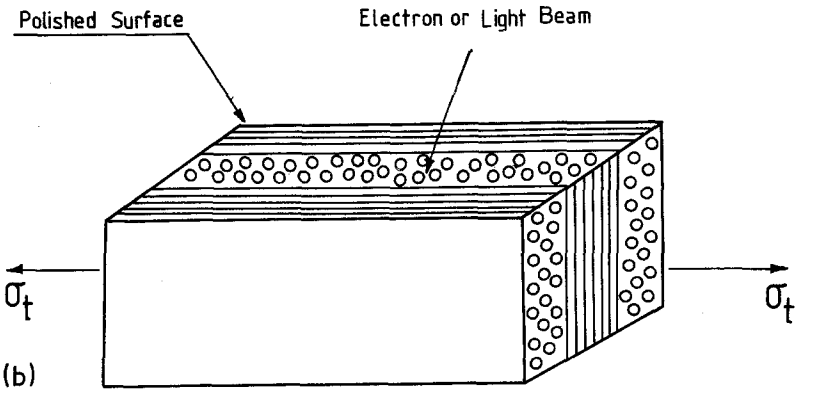


*Figure 1* (a) Cross-ply specimen model and (b) specimen orientation for SEM strain stage outside the microscope.

failure strain, $V_f$ was varied from 0.1 to 0.4 for polyester composites and from 0.35 to 0.6 for epoxy composites. The volume fractions used were restricted due to the different resin viscosities; the polyester was too viscous whilst the epoxy was highly fluid. The epoxy cross-ply laminates, however, had a volume fraction $V_f$ in the range of 0.55 to 0.65, whereas for the polyester cross-ply laminates $V_f = 0.4 \pm 0.03$.

The conventional tensile tests were carried out on a "TTD" model Instron machine using a cross-head speed of 0.5 mm min$^{-1}$. Specimens were parallel sided of 20 mm x 200 mm dimensions with ends being reinforced by GRP tabs in order to prevent their premature failure at the grips. 10 mm long strain gauges were bonded to the specimen surfaces to give measurement of strain. Both 90° unidirectional and 0°/90°/0° epoxy cross-ply laminates with a 90° ply thickness $2d = 2$ mm and outer ply thickness $b = 0.5$ mm on each side were tested, see Fig. 1a; the equivalent figures for the polyester laminates were $b = 0.7$ mm and $d = 0.6$ mm. The unidirectional laminates were loaded to failure and their failure strain was recorded as a function of $V_f$. The cross-ply laminates, however, were loaded up to a strain level just above their whitening strain of ~ 0.3% and were repeatedly loaded–unloaded for 3 to 4 cycles at that strain. They were then removed, annealed for about 15 min at 100° C and loaded again to the same maximum strain level. After a few cycles, the maximum strain level was raised

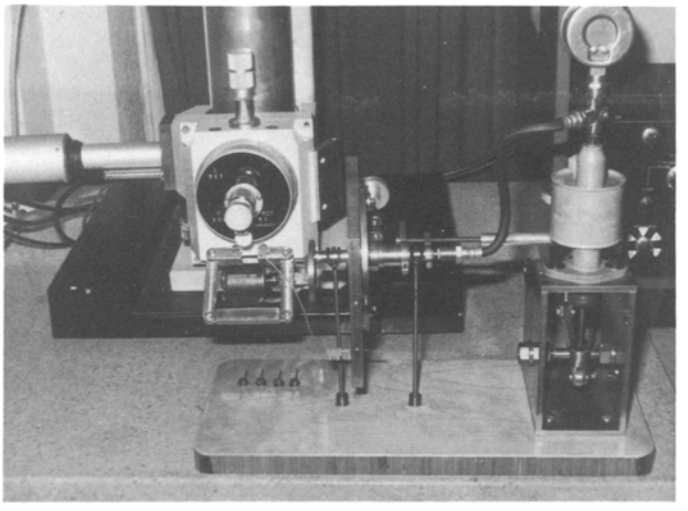

*Figure 2* The SEM strain stage outside the microscope.

to a higher value but a value still below the transverse cracking strain of about 0.55%. The specimen was under close visual observation for any signs of change in its appearance throughout the test.

Specimens for tensile tests on the scanning electron microscope (SEM) strain stage were model cross-ply laminates, shown in Fig. 1b, of 5 mm x 60 mm dimensions (30 mm gauge length). A 3 mm long electrical strain gauge was affixed to the specimen surface and strain was read by a portable strain indicator. The thin cross-sections (perpendicular to the fibre direction in the outer 0° plies) on both sides of the specimen were carefully polished down with 1 $\mu$m diamond paste for microscope observations. Polishing of both side faces was found necessary as otherwise failure would inevitably start from the unpolished face due to the damage induced during the cutting process. Specimens were coated in vacuum with a layer of gold/palladium alloy in order to render the surface electrically conducting. These laminates had plies of thickness 0.3 mm. In this geometrical region, transverse cracking is "constrained" as described elsewhere [3, 4], thus allowing a higher cracking strain and a controlled crack propagation mode beneficial for the study of the cracking behaviour.

In the tests with strain stage, an area of specimen was selected and photographed as the reference area throughout loading. The laminate was then slowly loaded, and loading was interrupted at about 0.05% strain increments for the area to be re-focused and photographed. This procedure was continued until a substantial amount of damage had occurred in the laminate. The specimen was then unloaded and was photographed in the totally unloaded state.

The SEM strain stage which is shown in Fig. 2 is operated by a hydraulic loading system. The device has been described in detail elsewhere [2]. The specimens were clamped between the frictional grips on the loading frame and were loaded into the SEM specimen chamber. The load was applied through a screw-driven hydraulic loading unit mounted outside the microscope. A pressure gauge was used to monitor the pressure applied to the actuator. Rotational and sliding "O" rings were also operated to give specimen movement along the three principal directions.

In addition to the above experiments, curing and thermal strains which are produced in the 0°/90°/0° laminate during fabrication were also measured for both epoxy and polyester systems. This was done as described elsewhere [4] by using 0°/90° unbalanced laminates having a ply thickness of 0.23 mm and 0.29 mm for the epoxy and polyester samples, respectively; the $V_f$ values for these laminates were similar to those of the cross-ply laminates. These 0°/90° laminates were cured under the same conditions as the 0°/90°/0° cross-ply laminates. Upon cooling from the curing temperature the unbalanced laminates bent. The radius of curvature was measured and the thermal strains were then calculated from the appropriate relationship [5].

## 3. Results

### 3.1. Tensile tests on 90° unidirectional laminates

Fig. 3a shows the failure strains of the unidirec-

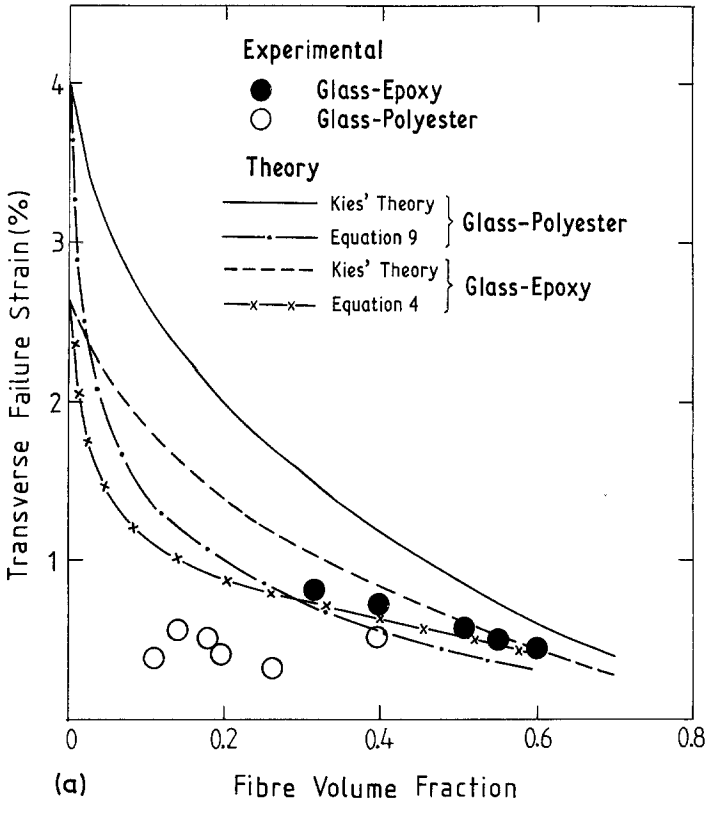


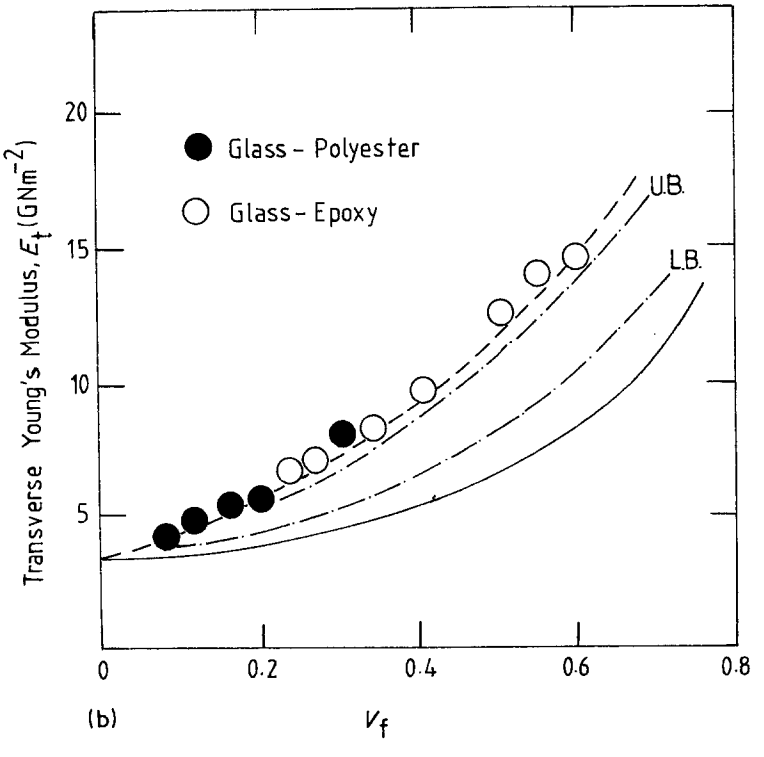


*Figure 3* (a) Comparison of the theoretical predictions and experimental results of the transverse failure strain of the unidirectional composites with fibre volume fraction and (b) comparison of experimental and theoretical values of transverse Young's modulus of the unidirectional composites as a function of fibre volume fraction, (——) Rule of Mixtures (Reuss bound), (—·—) Hashin–Rosen bounds, (----) Halpin–Tsai estimate.

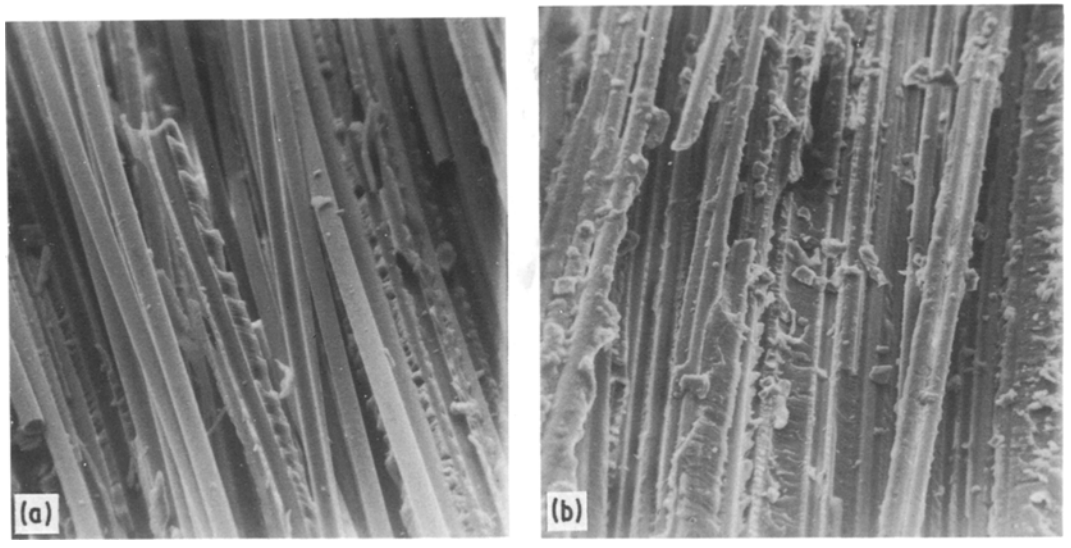


*Figure 4* Scanning electron micrographs of the fractured surface of the transverse unidirectional composites in (a) glass fibre/polyester system, showing clean surface of fully debonded fibres (× 235), and (b) glass fibre/epoxy system showing some resin still attached to the fibre surface (× 148).

tional laminates plotted as a function of the fibre volume fraction. It is noted that the failure strains of the epoxy composites fall with increasing $V_f$, whilst in polyester laminates, the failure strain is almost invariant at a value of 0.4%. It is worthwhile mentioning that the fibres in epoxy composites, particularly at higher $V_f$, were found to be much more uniformly distributed than those in the polyester laminates. This non-uniform fibre distribution leads to high local stress fields and may in part be responsible for the lower failure strain of polyester composites.

The experimental values of the transverse Young's modulus ($E_t$) are given in Fig. 3b for both epoxy and polyester laminates.

Studies of fracture surfaces of these laminates by SEM showed a stronger fibre–resin bond in the epoxy case. This is demonstrated in Fig. 4a and b where fibres in the polyester laminate show a clean surface whilst some quantities of resin are still found attached to the fibres in the epoxy composites.

## 3.2. Cyclic tensile tests on 0°/90°/0° cross-ply laminates

A typical stress–strain curve of a 0°/90°/0° epoxy cross-ply laminate with a relatively thick 90° ply is shown in Fig. 5. This curve shows two "knees" as reported previously [1]. The first "knee" occurring at ~ 0.25% was found to be associated with a visual "whitening" phenomenon in the specimen. The second "knee", however, was due to the onset of transverse cracking in the 90° ply at a strain of about 0.55%. The tensile strain in the 90° ply induced during curing and cooling of the laminate was measured from the radius of the curvature of a 0°/90° laminate and found to be 0.08%. This strain when added to the measured cracking strain of 0.55% gives a total value of 0.6% for the transverse cracking strain.

During cyclic loading of a specimen to a maximum strain below its transverse cracking, the whitening effect was found to partially disappear when unloading the laminate. The "knee" in the

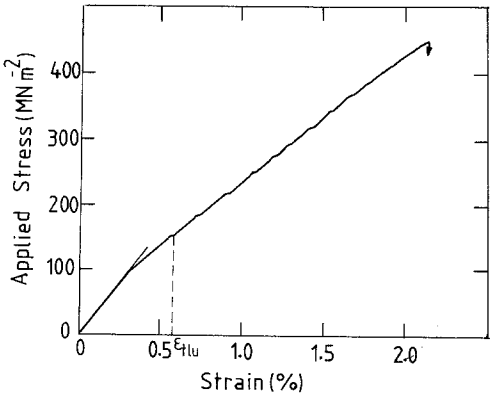


*Figure 5* Typical stress–strain curve of a 0°/90°/0° glass fibre/epoxy laminate showing two "knees". The first "knee" occurring at ~ 0.3% strain is associated with the visual whitening effect while the second "knee" is due to the cracking of the transverse ply at ~ 0.55% strain.

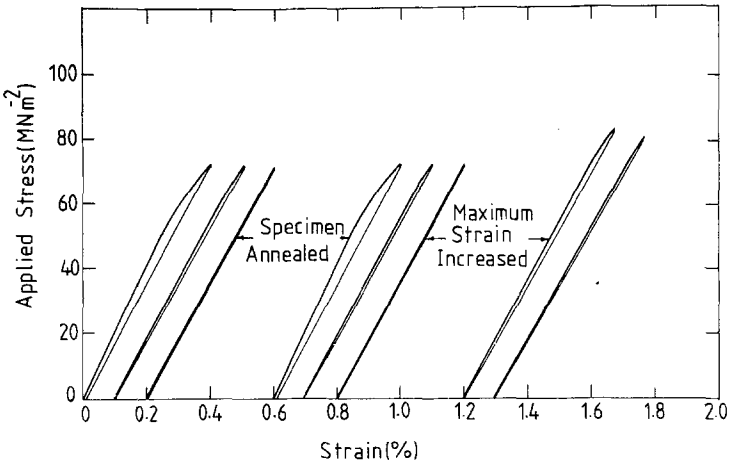


*Figure 6* Load–unload curves for 0°/90°/0° glass fibre/epoxy composites showing the disappearance of the non-linearity after a few cycles of loading. Annealing of the loaded specimen restores the pre-loading properties. Increasing the maximum strain level results in a "knee" when strain exceeds the previous maximum level.

curve also gradually vanished and the slope reduced during the first 3 to 4 cycles, see Fig. 6. The specimen was then removed from the grips and annealed as described above; this anneal caused a complete disappearance of the "whitening" effect. Upon reloading, the annealed composite behaved exactly like an "as new" specimen with the "whitening" and the "knee" both appearing at the same strains as observed in a new specimen. Increasing the maximum strain level produced new whitening and non-linearity in the stress–strain curve at strains greater than the previous maximum level.

Cross-ply laminates made from the polyester resin behaved differently, see Fig. 7. In this case, neither the whitening effect nor the accompanying knee were present. It should be noted however that these composites have a more translucent appearance as made. The curing and thermal strain in the 90° ply had a much greater value of ~ 0.25% which when added to the measured transverse cracking strain of 0.2% gives a total cracking strain of 0.45% which is close to the value of 0.4% observed for $\epsilon_{tu}$ in unidirectional laminae. Structural studies by optical microscopy of the polyester laminate prior to loading revealed some microcracks in the 90° ply, see Fig. 8. These cracks could have formed under large thermal strains present in the laminates.

### 3.3. Tensile tests in SEM

Figs 9 to 15 show the same selected area of an epoxy laminate specimen configuration as shown in Fig. 1b prior to loading and in the strained position with strains up to ~ 0.75%. Comparisons of these micrographs indicate the failure of the

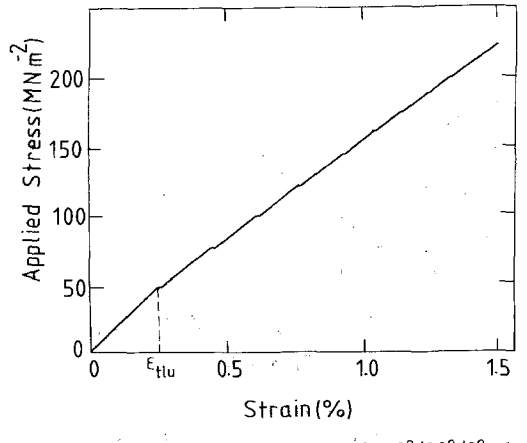


*Figure 7* Typical stress–strain curve of a 0°/90°/0° glass fibre/polyester laminate showing a "knee" associated with cracking in the transverse-ply at ~ 0.2% strain.

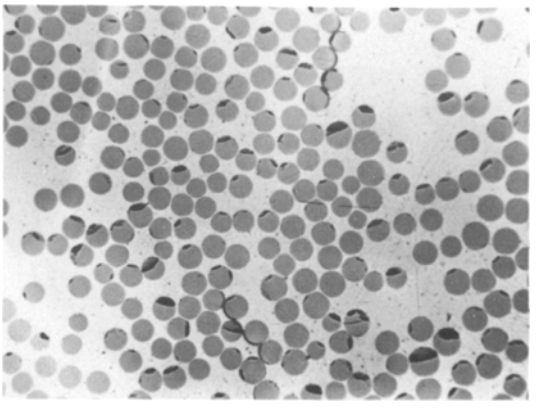

*Figure 8* Scanning electron micrograph showing the transverse microcracks in an untested 0°/90°/0° glass fibre/polyester cross-ply laminate. These cracks have formed due to the residual thermal strains (× 250).

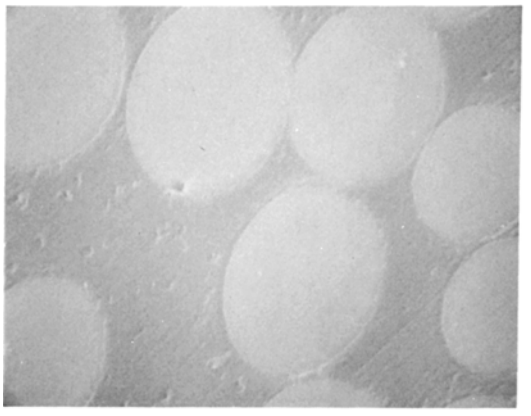

*Figure 9* Scanning electron micrograph of the selected area of the 0°/90°/0° glass fibre/epoxy cross-ply laminate prior to loading (X 2150).

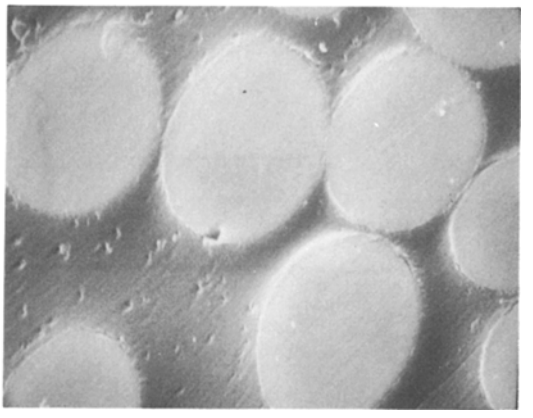

*Figure 11* Specimen at 0.3% strain. Both the debonding crack and the brightening effect are clearly observed (X 2150).

fibre–resin bond at strains between 0.1 and 0.3%, see Figs 10 and 11. Fibre debonds appear as cracks at a small angle to the loading axis. These cracks appear bright at the edges which is due to more secondary electrons being emitted at these areas. The gaps between fibre and resin open up considerably with increasing load with more fibres debonding from the resin. Another brightening effect is also observed at the portions of the boundaries almost perpendicular to the loading axis. This effect is considered to be due to the edges of fibres standing out of the surface of resin caused by the differential contractions of the two components. Clearly the bright lines will only appear on the side where the collector is placed.

At about 0.4% strain, see Fig. 12, some of the individual fibre debonds begin to link up, thus forming tiny cracks of two or three fibre diameters in length. Further coalescence of these cracks occurred at higher strains, see Figs 13 to 15. In Fig. 14, a low magnification photomicrograph of the specimen is also shown. This micrograph indicates some fibre fractures in both 0° and 90° plies in addition to the fibre debonds. These fibre fractures occurred at early stages of loading and are believed to be due to the damage induced during the surface preparation since fewer fibre fractures were seen in the better polished specimens.

Fig. 16 shows the specimen after being unloaded from ~ 0.75% strain. It is interesting to note that all the individual fibre debonds and fibre fractures appear to have closed up after unloading and only those small cracks formed by the coalescence of fibre debonds remain just visible.

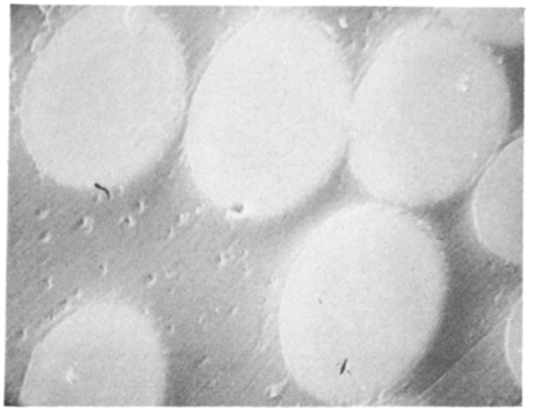

*Figure 10* Onset of fibre–matrix debonding at ~ 0.1% strain. Debonding is occurring on top of the fibre in the bottom right of the photograph. Some brightening effect is also seen on the left hand side of the fibres (X 2150).

## 4. Discussion

### 4.1. Transverse failure mechanism

Results obtained from the tensile tests on the strain stage clearly show that in 0°/90°/0° glass fibre reinforced epoxy laminates, fibre–matrix debonding precedes the transverse cracking of the 90° ply. Fibre debonding occurs at strains as small as 0.1% and increases with loading. At 0.3% strain, the effect becomes visual and is seen as a whitening phenomenon which is accompanied by a "knee" in the stress–strain curve, shown in Fig. 5. This whitening effect is considered to be due to the scatter of the light by the gaps which are generated between fibres and resin where fibres debond. Unloading results in closing up of these gaps but no rebonding occurs at room temperature.

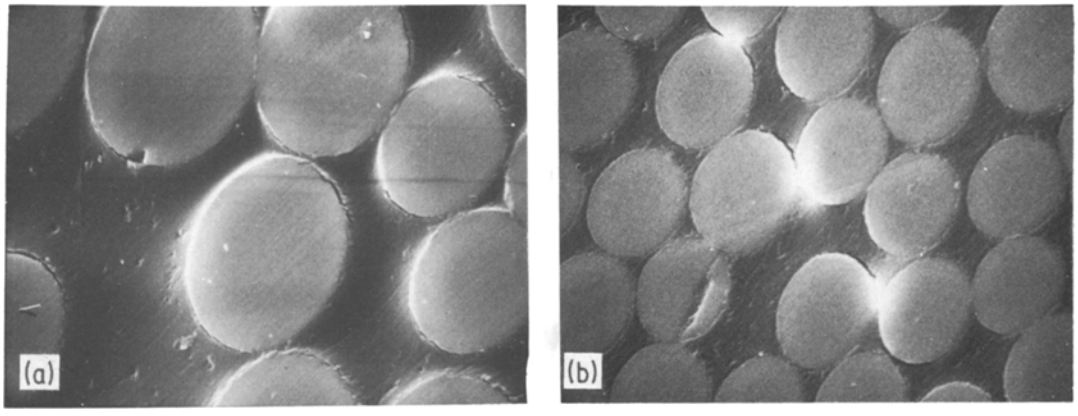


*Figure 12* Specimen at 0.4% strain; (a) fibre debonding in the selected area (× 2150), and (b) coalescence of fibre debonds occurring away from the selected area (× 1290).

Therefore, in the unloaded specimen, the whitening effect partially disappears but the modulus does not recover. By annealing the specimen at higher temperatures, fibres are found to rebond thus resulting in the complete disappearance of the whitening effect and recovery of the Young's modulus, Fig. 6. It should be stressed that this effect may not necessarily occur with all resin systems and fibre finishes. As the strain is increased, fibre debonds join up to form the nuclei for transverse cracks; the transverse cracks then develop by the coalescence and growth of these nuclei.

It is worthwhile mentioning that in these experiments a constrained laminate has been used in which crack propagation is controlled [3, 4]. In an unconstrained specimen, as soon as the crack nucleus is formed, it may propagate instantaneously and it would not be possible therefore to follow the crack path as it is forming.

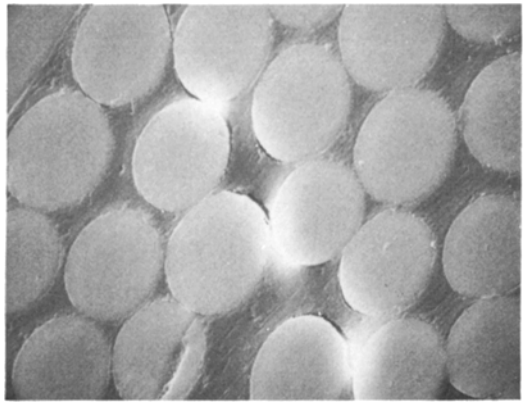

*Figure 13* Fibre debonds at ~ 0.5% strain (× 1290).

## 4.2. Effect of thermal strain on fibre debonding

The whitening effect and the accompanying "knee" in the stress–strain curve which is observed in the epoxy cross-ply composites has not been detected in similar polyester laminates. This may be due to the effect of the thermal strain generated during fabrication.

The experiments carried out to determine the thermal strain, $\epsilon_{tl}^{th}$, generated in the transverse ply in the longitudinal direction gave a value for the polyester laminate of 0.25% compared with a value of 0.08% for the epoxy laminate. The actual average strain for the visual debonding or whitening is 0.3% for the epoxy system which when added to the thermal strain of 0.08% gives a total of 0.38% for debonding. If it is assumed that the actual debonding strain for the polyester system is similar to that for the epoxy system, then the whitening should be observed at ~ 0.13% which is obtained by subtracting the thermal strain of 0.25% from 0.38%. Clearly if bonding is weaker in the polyester system then debonding will occur with the action of the thermally generated strain and the whitening effect will therefore be absent. Transverse microcracks in the polyester system have been observed prior to loading, see Fig. 8. It can be deduced therefore that the debonding strain for the glass fibre polyester system investigated is less than 0.25% compared with a value of ~ 0.4% for the epoxy system used.

## 4.3. Mechanism of rebonding (recovery effect)

Clearly two requirements must be fulfilled for the rebonding of fibres and matrix to fully eliminate

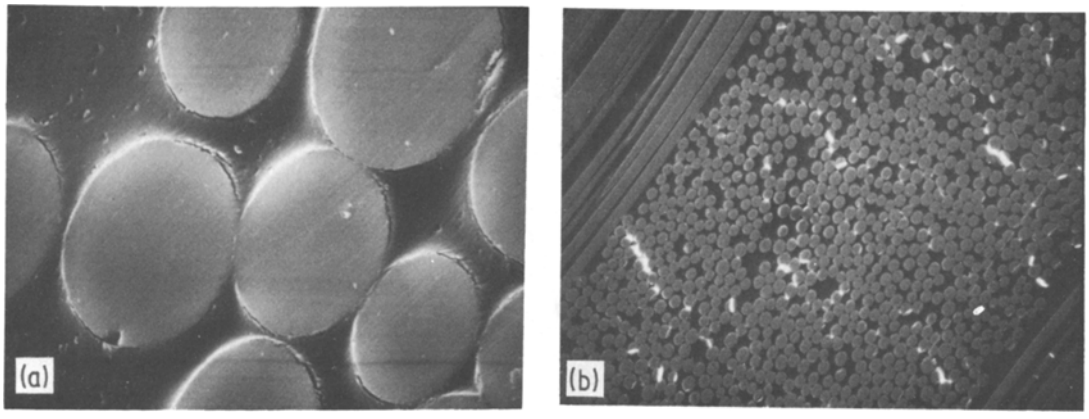


*Figure 14* Extent of damage at ~ 0.6% strain. (a) the selected area (× 2150), (b) low magnification photomicrograph of the specimen; the bright regions correspond to fibre debonds and fibre fractures (× 130).

the whitening effect. Firstly, the thermal strain must be recovered in order to allow the two surfaces to come together again. Secondly, chemical reaction must occur to permit rebonding. In the experiments carried out here, recovery occurred at ~ 100° C for the epoxy system and therefore this temperature is sufficiently high to reduce the thermal strains to zero. It cannot be deduced from the experiments whether or not a temperature as high as 100° C is necessary for recovery to occur.

### 4.4. Prediction of the transverse-ply's failure strain

Results of tensile tests on unidirectional 90° laminae show that failure strain drops with increasing $V_f$ for epoxy laminates but for the polyester system it remains almost constant ~ 0.4%, see Fig. 4. In Fig. 4, the experimental results are compared with Kies' theoretical values [6]. Kies' values are shown to overestimate the failure strain in both systems particularly at low $V_f$. This is due to the fact that Kies [6] assumes both a regular fibre array with an effective $V_f$ that is higher than the average and perfect bonding. These two conditions are not met in real composites where fibre clustering is often present, particularly at low $V_f$. The clustered regions have a Young's modulus greater than that of the low $V_f$ areas and they therefore carry a larger portion of the load. These high local stress fields therefore result in premature failure initiating in the clustered regions. Kies' model also ignores the stress concentration generated in the matrix due to the presence of the stiffer fibres. An attempt has been made to marry the Kies strain magnification theory with the stress concentration and apply the results to the real composites. In the model considered here, fibres are assumed to be randomly distributed in such a way that the

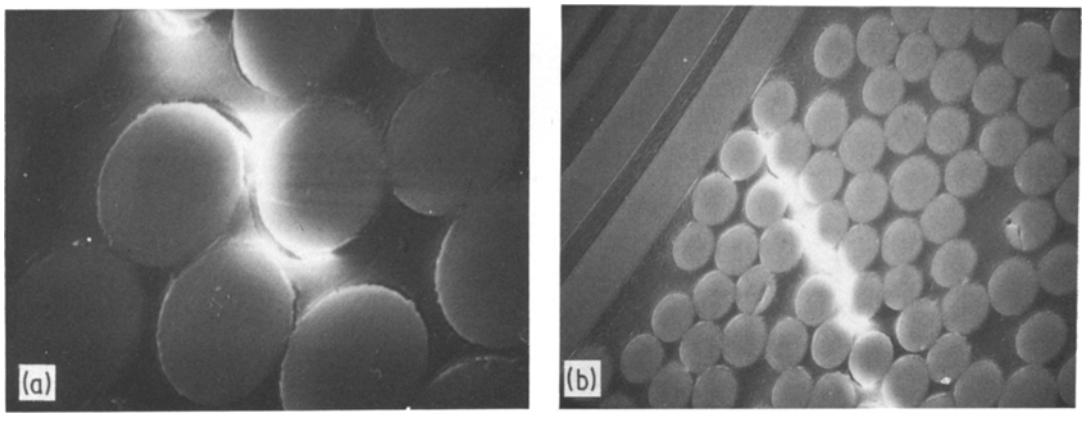


*Figure 15* (a) High magnification (× 1720) and (b) low magnification micrographs taken at 0.75% strain of the region where fibre debonds have joined up (× 860).

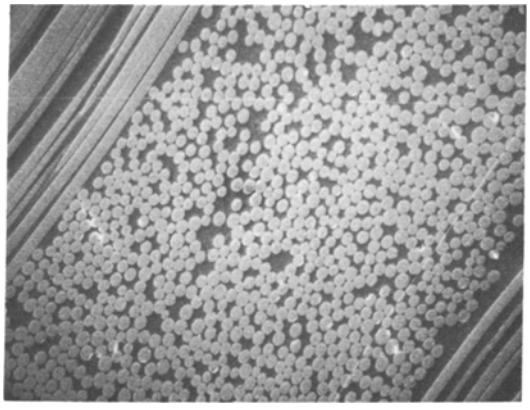

*Figure 16* Low magnification micrograph of the specimen after being unloaded showing a close-up of the fibre debonds and fibre fractures previously observed (× 130).

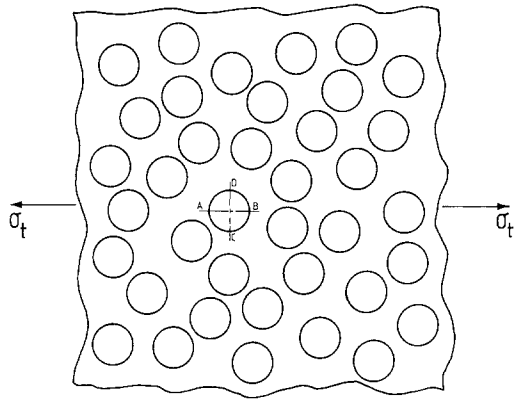


*Figure 17* Model for the random fibre distribution. It is assumed that $V_f$ along any line is equal to the average $V_f$ of the composite.

average concentration of fibres is the same along any line parallel or perpendicular to the specimen axis and it is equal to the average $V_f$, see Fig. 17.

Two cases can be considered. First, fibres are bonded and they therefore carry load, and second, fibres are not bonded and therefore they do not contribute directly to load carrying.

When fibres are bonded, as for the epoxy system, the simple Reuss model (in parallel coupling) gives the transverse modulus $E_t$ as

$$\frac{1}{E_t} = \frac{V_m}{E_m} + \frac{V_f}{E_f}, \tag{1}$$

where $V_f$ is the experimental fibre volume fraction, $E_m$ and $E_f$ are the Young's moduli of the matrix and fibre respectively and $V_m = (1 - V_f)$. As shown in Fig. 3b this model does not fit the experimental results. Also shown in Fig. 3b are the Hashin–Rosen bounds [7] and the Halpin–Tsai estimate [8]; it is to be noted however that both epoxy and polyester laminates fit the latter well. Note that one theoretical curve is expected to fit within the accuracy of the test results because $E$ values for the polyester and epoxy matrices are almost identical, i.e. 3.45 and 3.6 MW m$^{-2}$ respectively. For an overall transverse ply stress $\sigma_t$, the maximum local stress in the matrix is given by

$$(\sigma_m)_{max} = K\sigma_t, \tag{2}$$

where $K$ is the maximum stress concentration factor in the resin at points A and B in Fig. 17.

The composite fails when $(\sigma_m)_{max}$ reaches the matrix failure stress $\sigma_{mu}$. Thus from Equation 2

$$\sigma_{tu} = \frac{\sigma_{mu}}{K}, \tag{3}$$

where $\sigma_{tu}$ is the failure stress of the transverse ply.

From Equation 3 and putting $\sigma_{mu} = \epsilon_{mu}E_m$ the transverse ply failure strain $\epsilon_{tu}$ is given by

$$\epsilon_{tu} = \frac{\epsilon_{mu}E_m}{KE_t}. \tag{4}$$

Values of $\epsilon_{tu}$ have been calculated from Equation 4 for $K = 2.0$ and are plotted in Fig. 3b as a function of $V_f$ for the epoxy system. Comparison shows that these approximate theoretical values give reasonable agreement with the experimental results. The Kies prediction effectively assumes that Equation 1 is applicable and uses a higher $V_f$ to improve the fit.

When fibres are not bonded, as is likely to be the case for the polyester system, load is only carried by the matrix. Thus

$$\sigma_t = V_m\sigma_m \tag{5}$$

where $\sigma_m$ is the overall matrix stress.

The presence of the fibres produces a stress concentration $K'$ in the matrix at the points C and D in Fig. 17. The maximum stress in the matrix is therefore given by

$$(\sigma_m)_{max} = K'\sigma_m \tag{6}$$

where $K'$ is the maximum stress concentration factor. The composite fails when $(\sigma_m)_{max}$ equals $\sigma_{mu}$ and therefore, when using Equation 6,

$$\sigma_m = \frac{\sigma_{mu}}{K'} \tag{7}$$

is obtained. Therefore from Equations 5 and 7, the overall composite failure stress $\sigma_{tu}$ is given by

$$\sigma_{tu} = \frac{\sigma_{mu} V_m}{K'} . \quad (8)$$

Equation 8 can be expressed in terms of strain as follows

$$\epsilon_{tu} = \frac{\epsilon_{mu} V_m}{K'} \frac{E_m}{E_t} . \quad (9)$$

Values of $\epsilon_{tu}$ have been calculated from Equation 9 using a value of 2 for $K'$ for the polyester system and are shown in Fig. 3a. These values are found to give a better approximation to the experimental results, however the discrepancy between the simple theory and experiment may be due either to the use of an incorrect value of $K'$ for the composite or because cracks have been introduced into the comparatively brittle polyester laminate during the preparation of the sample for testing.

It should be pointed out that in these oversimplified models specific values of $K$ and $K'$ will reduce to 1 at $V_f = 0$ and the values used at finite $V_f$ will depend on the arrangement of fibres in the composite (see for example Daniel [9] and Chamis [10]). Although we observed fibre bunching in our composites, we have assumed a constant value for $K$ of 2.0 (obtained from Equation 12 given by Chamis [10]) and $K' = 2.0$.

## 5. Conclusions

Straining stage experiments on the 0°/90°/0° glass fibre epoxy cross-ply laminates have shown that fibre debonding occurs in the transverse-ply at strains at which both the visual whitening effect and small modulus changes are observed. It is concluded therefore that the whitening effect is associated with fibre debonding.

Annealing experiments show that, for the glass fibre epoxy system, thermal annealing at ~ 100° C in the absence of stress enables the fibre to rebond thereby producing an "as new" composite.

In contrast the glass fibre polyester system studied does not show a whitening effect or associated modulus change at strains below the transverse cracking strain. Furthermore, thermal strains generated in these composites were much greater than for the glass fibre epoxy system and scanning electron microscopy studies revealed evidence of debonded fibres in the "as-formed" composites. It is concluded that these observations strongly support the view that for the polyester system, thermal strains generated on annealing from the curing temperature cause debonding and that the composites are therefore effectively whitened before stress is applied.

It is shown that using simplified theoretical arguments it is possible to explain the observed dependence of transverse tensile strength on $V_f$ of both the glass epoxy and glass polyester systems on the assumption that fibres are bonded in the former and not bonded in the latter.

The strain stage experiments in the scanning electron microscope also demonstrate that transverse cracks form by the coalescence and growth of fibre debonds in the composite. These observations were made possible by using geometric configurations that lead to constrained cracking [3] thereby allowing crack nucleation and crack propagation to be separated.

## Acknowledgment

It is a pleasure to acknowledge discussions with our colleague Mr M. G. Bader.

## References

1. A. PARVIZI and J. E. BAILEY, *J. Mater. Sci.* **13** (1978) 2131.
2. M. I. MANNING and P. J. GOODHEW, *J. Phys. E: Sci. Instrum.* **12** (1979) 464.
3. A. PARVIZI, K. W. GARRETT and J. E. BAILEY, *J. Mater. Sci.* **13** (1978) 195.
4. J. E. BAILEY, P. T. CURTIS and A. PARVIZI, *Proc. Roy. Soc. Lond.* **A366** (1979) 599.
5. R. M. BRAND and S. BARKER, *J. Text. Res.* **32** (1962) 39.
6. J. A. KIES, US Naval Research Lab. Rep. No. 5752 (1962).
7. Z. HASHIN and B. W. ROSEN, *J. Appl. Mechanics, Trans. ASME* **31** (1964) 223.
8. J. G. HALPIN and S. W. TSAI, *AFML-TR 67-423*, June 1969.
9. J. M. DANIEL, in "Composite Materials", Vol. 2, edited by L. J. Broutman, R. H. Krock and G. P. Sendeckyj (Academic Press, New York, 1974) Ch. 10.
10. C. C. CHAMIS, in "Composite Materials", Vol. 5, edited by L. J. Broutman and R. H. Krock (Academic Press, New York, 1974) Ch. 3.

Received 28 July and accepted 1 August 1980.